tvst

Article

Drug Tissue Distribution of TUDCA From a Biodegradable Suprachoroidal Implant versus Intravitreal or Systemic Delivery in the Pig Model

Timothy W. Olsen[1,3], Roy B. Dyer[2], Fukutaro Mano[1], Jeffrey H. Boatright[3], Micah A. Chrenek[3], Daniel Paley[4], Kathy Wabner[5], Jenn Schmit[3], Ju Byung Chae[3,6], Jana T. Sellers[3], Ravinder J. Singh[2,7], and Timothy S. Wiedmann[4]

[1] Department of Ophthalmology, Mayo Clinic, Rochester, MN, USA
[2] Division of Clinical Biochemistry and Immunology, Mayo Clinic, Rochester, MN, USA
[3] Department of Ophthalmology, Emory University School of Medicine, Atlanta, GA, USA
[4] Department of Pharmaceutics, University of Minnesota, Minneapolis, MN, USA
[5] Department of Civil Engineering, University of Minnesota, Minneapolis, MN, USA
[6] Department of Ophthalmology, Chungbuk National University, Chungbuk, South Korea
[7] Department of Laboratory Medicine and Pathology, Mayo Clinic, Rochester, MN, USA

Correspondence: Timothy W. Olsen, Department of Ophthalmology, Mayo Clinic, 200 First Street SW, Rochester, MN 55905, USA. e-mail: olsen.timothy@mayo.edu

Received: December 16, 2019
Accepted: March 10, 2020
Published: May 15, 2020

Keywords: bile acid; drug delivery; pharmacokinetics; retinal degeneration

Citation: Olsen TW, Dyer RB, Mano F, Boatright JH, Chrenek MA, Paley D, Wabner K, Schmit J, Chae JB, Sellers JT, Singh RJ, Wiedmann TS. Drug tissue distribution of TUDCA from a biodegradable suprachoroidal implant versus intravitreal or systemic delivery in the pig model. Trans Vis Sci Tech. 2020;9(6):11, https://doi.org/10.1167/tvst.9.6.11

Purpose: To determine local ocular tissue levels of the bile acid, tauroursodeoxycholic acid (TUDCA), in the pig model using oral, intravenous (IV), intravitreal injection (IVitI) and low- and high-dose suprachoroidal, sustained-release implants (SCI-L or SCI-H).

Methods: Forty-six pigs (92 globes) were included in the study. TUDCA was delivered orally in 5 pigs, IV in 4, IVitI in 6, SCI-L in 17, and SCI-H in 14. Testing timeframes varied from the same day (within minutes) for IV; 1 to 6 days, oral; and 1 to 4 weeks, IVitI and SCI. Enucleated globes were dissected, specimens from specific tissues were separated, and TUDCA was extracted and quantified using mass spectrometry.

Results: The highest TUDCA tissue levels occurred after IV delivery in the macula (252 $\pm$ 238 nM) and peripheral retina (196 $\pm$ 171 nM). Macular choroid and peripheral choroid levels were also high (1032 $\pm$ 1269 and 1219 $\pm$ 1486 nM, respectively). For IVitI delivery, macular levels at day 6 were low (0.5 $\pm$ 0.5 nM), whereas peripheral choroid was higher (15.3 $\pm$ 16.7 nM). Neither the SCI-L nor SCI-H implants delivered meaningful macular doses ($\leq$1 nM); however, peripheral retina and choroid levels were significantly higher. Bile acid isoforms were found in the serum specimens.

Conclusions: The highest TUDCA tissue levels in the pig model were obtained using IV delivery. Oral delivery was associated with reasonable tissue levels. Local delivery (IVitI and SCI) was able to achieve measurable local ocular tissue levels.

Translational Relevance: Diffusional kinetics from the suprachoroidal space follow the choroidal blood flow, away from the macula and toward the periphery.

Introduction

Diseases and degeneration of the neurosensory retina, photoreceptors, retinal pigment epithelium (RPE), and choroid are numerous and may lead to substantial loss of vision or blindness.[1,2] *Retinitis pigmentosa* is a broad term used to represent genetic-based photoreceptor disorders. Treatments for such posterior segment ophthalmologic disorders include surgery, laser-based therapy,[3] pharmacotherapy,[4–9] and, more recently, gene therapy. In addition to gene therapy, there is now a role for a mechanical retinal prosthesis for those with end-stage disease.[10]

Local drug delivery methods, which are used to treat a variety of ophthalmologic conditions, avoid or minimize systemic toxicity. Topical therapy is primarily used for anterior-segment conditions, whereas

intravitreal injections (IVitIs) are well established for posterior-segment disorders. Advantages of IVitI include ease of delivery, repeatability, and low systemic drug levels. Although drugs used in intravitreal therapy may be expensive, their low delivery cost is a key advantage. More recently, a suprachoroidal microcannulation technique has been described and studied by multiple investigators.[11–16] The pharmacodynamic implications for suprachoroidal drug delivery are being clarified as pharmacokinetic measurements are coupled with a pharmacologic effect. In the pig model, triamcinolone, suspended in an appropriate excipient, can be localized in the suprachoroidal space and can provide sustained local tissue delivery.[12] However, our group[13] showed that the use of the biologic agent bevacizumab in the suprachoroidal space had only a transient local half-life and rapidly entered the systemic circulation.

IVitI of small molecules, especially biologic agents, has become the primary method for safe and effective delivery of intraocular pharmacotherapies to the posterior segment of the eye. Regular monthly IVitIs are commonly used for chronic disorders such as neovascular age-related macular degeneration.[17] Although effective for anterior-segment disorders, drugs topically applied to the eye typically will not reach posterior-segment tissues in sufficient therapeutic concentrations because of regional blood flow as well as diffusion and aqueous flow kinetics. Therefore, topical medications have largely been ineffective for the treatment of primary posterior-segment disorders. Treatment of cystoid macular edema using topical agents is largely dependent upon successfully controlling anterior-segment inflammation. Despite the clear benefits of intravitreal delivery, the rapid diffusion of drug shortens the duration of action, especially for biologic agents such as those targeting vascular endothelial growth factor.[4–6] More recently, methods that introduce drugs into the suprachoroidal space have been described and may offer an alternative, sustained delivery to treat posterior-segment tissues.[11–14,18–22]

In 2002, Rodrigues et al.[23] studied the neuroprotective effect of the bile acid tauroursodeoxycholic acid (TUDCA) in a rat model of acute stroke. Subsequent studies suggested that the beneficial effects of TUDCA were due to inhibition of neural apoptosis[24] mediated by mitochondria-related signals.[25] Next, systemic injections of TUDCA in retinal-degeneration 10 and light-induced retinal degeneration mouse models were shown to suppress apoptosis in photoreceptor cells.[26] The protective effect of TUDCA on the retina has been confirmed by numerous investigators.[27–36]

For this study, we developed a slow-release, biodegradable, curved TUDCA implant that was surgically implanted into the suprachoroidal space in the pig model. Tissue concentrations of TUDCA were measured and compared to those obtained following IvitI, oral, and intravenous (IV) TUDCA administration. Although relative doses administered differed, doses were determined on the basis of known estimates to optimize local retinal tissue levels balanced with known, delivery-related adverse effects. Our target tissues included the neurosensory macula, peripheral retina, and the corresponding choroidal tissues.

Methods

The animal studies performed were approved by the Institutional Animal Care and Use Committee at Emory University in Atlanta, Georgia. Tissue analysis for pharmacokinetics was performed at Mayo Clinic in Rochester, Minnesota. Studies were conducted in accordance with the guidelines on conduct of animal experiments and experimental design as outlined in the Statement for the Use of Animals in Ophthalmic and Vision Research of the Association for Research in Vision and Ophthalmology. Our method of neural tissue drug extraction and quantitative analysis using mass spectroscopy techniques was adopted from Camilleri et al.[37]

Study Groups by Delivery Method

We studied 46 pigs ($N = 92$ globes) grouped by delivery method: oral ($n = 5$), IV ($n = 4$), IVitI ($n = 6$), and suprachoroidal implant (SCI, $n = 31$) divided into high-dose (SCI-H, $n = 14$) and low-dose (SCI-L, $n = 17$) groups.

Oral Delivery

Initially, we attempted to feed the TUDCA placed within a marshmallow to each animal. However, the animals only partially consumed the marshmallow, and the uptake of TUDCA was entirely unpredictable for days 1 ($n = 2$) and 2 ($n = 1$). However, after day 2, an oral dose of 1 g/d TUDCA or 70 mg/kg/d TUDCA was sprinkled on the morning chow for 5 ($n = 2$) days. Globes were obtained for analysis within 24 hours of the initial dose of TUDCA. On days 2 (unreliable delivery for one animal) and then on day 6 (reliable delivery), the animals ($n = 2$) had 1 g oral TUDCA daily, and both globes ($n = 4$ globes) were enucleated 12 hours after the final dose.

The TUDCA was sprinkled on moistened morning chow and completely consumed when the animals were hungry for each of the final 4 of 5 days, thus presum-

ably reaching a steady state. The most reliable oral data were therefore derived from the day 6 group, and these data are reported.

Delivery

In this group ($n = 4$), 1 g TUDCA was dissolved in normal saline, buffered to pH 7.0 at a final concentration of 50 mg/mL, and administered over approximately 20 minutes. The first pig's globes were processed immediately after IV dosing was complete (time [T] = 0), then one pig ($n = 2$ globes) at each of the following intervals after completion of the IV infusion: 5, 30, and 60 minutes.

Local Treatment

For all local treatments (IVitI and SCI), only the right globe was treated, but both globes were analyzed. Animals had general sedation and were treated as per previous protocols.[12,13,15]

IVitI Delivery

Each animal was anesthetized with the right eye prepared using topical 5% betadine solution, 1% atropine, topical proparacaine, and a sterile lid speculum. Using a sterile surgical technique, injections were performed using a 30-gauge needle on a tuberculin syringe through the pars plicata ($n = 6$). The concentration of 5 mg/mL with a 100-µL volume was used for each IVitI for a total TUDCA dose of 0.5 mg per eye (pH buffered to 7.2). Animals were humanely killed at approximately 1, 2, and 4 weeks after the IVitI.

Suprachoroidal Implant

Fabrication

TUDCA was dissolved in dimethylformamide either as a mass/volume or mass/mass solution. Polycaprolactone (PCL) and polyethylene glycol (10,000 g/mole molecular weight) in a 2:1 weight ratio were weighed and combined in a 20-mL scintillation vial with 10 to 15 mL chloroform. The dispersion was stirred at 40°C. Dimethylformamide was then added during vigorous stirring, the solution transferred to a petri dish, and solvents evaporated at room temperature for 2 days. The film was then placed between two evenly spaced glass plates, heated on a hot plate until melted, pressure applied to yield a uniform thickness, and then cooled. A 1-cm trephine cut the film into an oval wafer that was placed into a hemispherical concave mold contained in a water bath (80°C–100°C).

The PCL was placed in a Teflon hemispherical mold, heated (60°C–70°C), and then cooled to −18°C for 30 minutes. Two polymers were mixed by weight by dissolving in dichloromethane. The solution was dried completely in thin sheets to remove organic solvent, then cut and cast. Once the PCL softened, spheres were used to press the molten PCL (Fig. 1A) to achieve the desired shape and thickness (Fig. 1B). A circular trephine cut the film hemisphere to create a curvilinear disc (SCI; Fig. 1C). Drug concentration was 15 mg/mL for SCI-H and 4 mg/mL for SCI-L, or 1.1 mg/g and 9.4 mg/g by weight, respectively. Each SCI-H contained 164 μg, whereas SCI-L contained 44 μg TUDCA. We measured an expected release rate of TUDCA from the SCI device with a rapid "burst-effect" from the device surface, followed by a slower, sustained release as the drug slowly diffused through the polymer.

SCI Surgical Implantation Procedure

Each animal was anesthetized, the right eye was prepared according to standard surgical sterile protocol, and a conjunctival peritomy was performed to expose the sclera (Fig. 2A). A No. 69 surgical blade was used to create a circumlinear, full-thickness incision through the sclera to expose the underlying choroid. The suprachoroidal space was expanded using a viscoelastic agent (Healon; Johnson & Johnson, New Brunswick, NJ, USA). The conjunctiva was closed using an interrupted 6-0 plain gut suture (Ethicon, Cincinnati, OH, USA; Fig. 2B). The implant was rotated into the suprachoroidal space (Fig. 2C) and the sclerotomy closed using 7-0 Vicryl suture (Ethicon). A retrobulbar block of 0.75% bupivacaine, 40 mg triamcinolone (Kenalog; Bristol-Myers Squibb, New York, NY, USA), and 100 mg cefazolin were delivered into the subtenon space with a blunt cannula. Atropine drops (1%) and antibiotic ophthalmic ointment (erythromycin) were used at the conclusion of the case.

Implants were sterilized using ethylene oxide at 54°C. Each implant melted and slightly deformed from the original configuration. During implantation, implants were cut in half into a *D* shape. Thus, each SCI implant delivered only half of the originally projected dose. Drug concentration within the implants was measured along with specific tissue measurements.

All animals were anesthetized and then humanely killed with an overdose of pentobarbital sodium (100 mg/kg). Serum samples were centrifuged from whole blood.

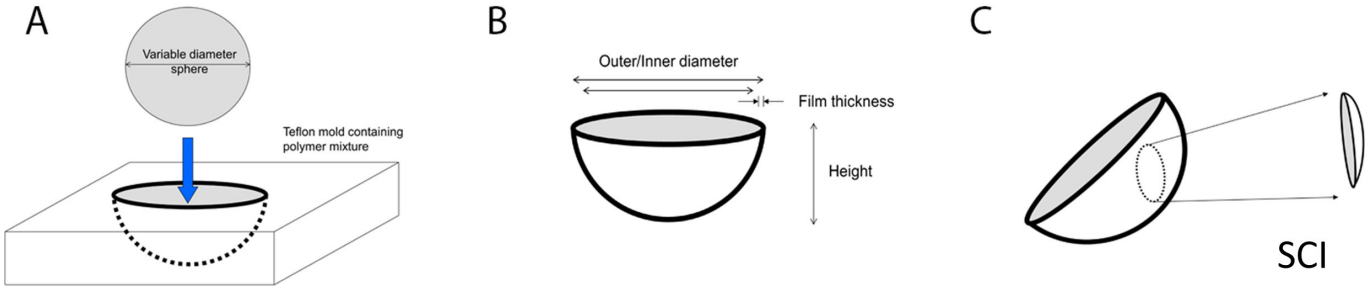

Figure 1. Creating the SCI. The polymer film molding process was used to create a suprachoroidal, sustained-release implant. (A, B) Drug-loaded polycaprolactone polymer was pressed by a metal sphere into a mold to form a hemispherical shell of prespecified thickness. (C) An oval trephine (1 cm) was used to cut the SCI from the hemispherical shell.

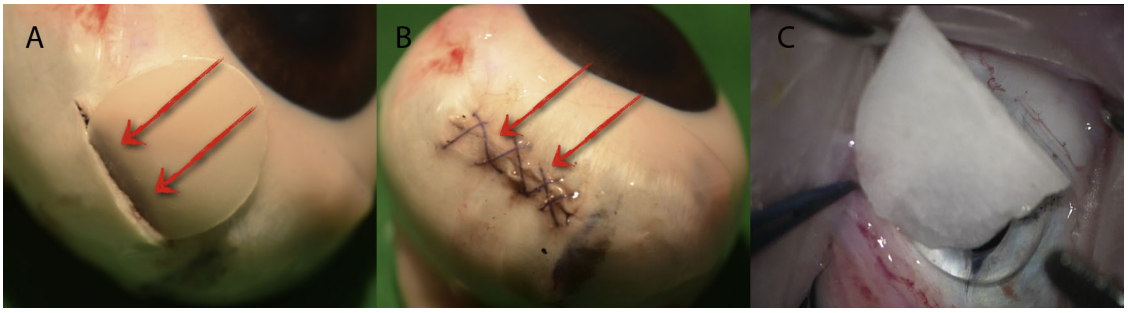

Figure 2. Insertion of the suprachoroidal implant. (A) Ex vivo. (B) Sutured. (C) In vivo.

Globe Dissection

Each globe was enucleated ($n = 2$ globes per pig) and specimens obtained within 5 to 10 minutes of death along with a blood sample. Enucleated globes were dissected into individual specimens, separated into labeled microfuge containers, and flash-frozen in liquid nitrogen. Anterior segments of each globe were removed using a razor blade (lens, cornea, and anterior segment), vitreous was removed separately, and a 2.5-mm trephine was used to obtain punch biopsies from the area centralis (macular equivalent in the pig), periphery (immediately over the SCI), and 180° away from the SCI and defined as residual retina or choroid. The neurosensory retina was separated from the underlying choroid Bruch's membrane and RPE (together) and stored as above.

Mass Spectrometry

Tissue was extracted in ethanol as previously described.[29] Dried extracts were reconstituted in methanol in a volume proportional to the tissue mass and analyzed by direct injection on liquid chromatography (LC)–mass spectrometry (MS)/MS in negative mode. Serum samples (100 µL) were mixed with 50 µL internal standard (IS) at 2 µM, and protein was precipitated by addition of 200 µL acetonitrile. Following filtration, 650 µL 80:20 H_2O/methanol was added. Extracts were resolved on a cohesive LC system (Cohesive Technologies, now Thermo Fisher Scientific, Waltham, MA, USA) and quantified on an Applied Biosystems 5000 triple quadrupole mass spectrometer (AB Sciex, Framingham, MA, USA). Tissue extracts were mixed with 2 µM IS (D5-TUDCA [deuterated TUDCA]) at a ratio of 4:1 (extract/IS), and 10 µL was injected. For extracted serum, 50 µL was injected. Analytes were resolved by reverse-phase gradient high-performance liquid chromatography on an Agilent Poroshell 120 EC-C10 column (2.7 µm; 2.1 × 50 mm) (Agilent, Santa Clara, CA, USA) with ramp gradient from 2% mobile phase A (5:95 methanol/H_2O, 10 mM ammonium acetate) to 98% mobile phase B (99:1 methanol/H_2O, 10 mM ammonium acetate) over 11 minutes. Before ramping, the column was equilibrated with 58% A/42% B. After gradient elution, the column was reequilibrated.

Statistical Analysis

Data were reported as mean ± standard deviation. Statistical analysis was performed using JMP 14 software (SAS Institute, Cary, NC, USA). Comparisons of drug levels between groups were assessed

Table 1. TUDCA Levels in Tissue Samples from the Right Eye

Delivery Method and Sample Time, Right Eye ($N = 45$)	Tissue Level, nM							
	Serum	Vitreous	Macula Retina	Macula Choroid	Peripheral Retina	Peripheral Choroid	Residual Retina	Residual Choroid
1 week								
Oral ($n = 2$)	230 ± 17.7	30.8 ± 6.0	2.3 ± 0.4	2.9 ± 0.4	1.9 ± 0.6	5.7 ± 2.1	2.4 ± 0.4	6.4 ± 1.0
IVitI ($n = 4$)	3.7 ± 2.5	16.1 ± 6.1	0.5 ± 0.5	1.3 ± 1.9	3.3 ± 5.2	15.3 ± 16.7	3.3 ± 4.5	19.1 ± 11.7
SCI-H ($n = 5$)	8.9 ± 5.9	7.1 ± 8.7	1.0 ± 0.8	0.6 ± 0.6	15.1 ± 15.3	137 ± 207	7.3 ± 12.1	10.4 ± 7.1
SCI-L ($n = 6$)	3.9 ± 5.7	6.0 ± 7.9	0.3 ± 0.2	0.3 ± 0.3	1.4 ± 1.4	3.0 ± 3.4	0.8 ± 0.5	1.4 ± 1.0
2 weeks								
IVitI ($n = 4$)	9.1 ± 4.8	12.9 ± 15.3	0.3 ± 0.4	0.9 ± 0.5	0.4 ± 0.5	1.2 ± 1.5	0.1 ± 0.1	6.0 ± 2.3
SCI-H ($n = 4$)	45.4 ± 49.2	0.8 ± 0.2	0.1 ± 0.2	0.3 ± 0.2	0.9 ± 0.6	5.8 ± 4.6	0.9 ± 0.9	2.7 ± 2.9
SCI-L ($n = 7$)	34.4 ± 45.6	3.9 ± 4.0	0.3 ± 0.5	0.5 ± 0.6	0.8 ± 0.6	2.4 ± 1.9	0.3 ± 0.3	2.2 ± 2.2
4 weeks								
IVitI ($n = 4$)	4.6 ± 4.6	8.3 ± 4.2	0.2 ± 0.2	0.7 ± 0.6	0.1 ± 0.3	0.5 ± 0.4	0.3 ± 0.3	3.0 ± 1.3
SCI-H ($n = 5$)	27.4 ± 35.3	1.6 ± 1.6	0.1 ± 0.2	0.2 ± 0.3	0.2 ± 0.2	0.5 ± 0.6	0.2 ± 0.2	0.5 ± 0.6
SCI-L ($n = 4$)	5.5 ± 3.8	1.4 ± 0.5	0.2 ± 0.2	0.1 ± 0.1	0.1 ± 0.1	0.5 ± 0.6	0.2 ± 0.2	0.4 ± 0.2

Data are shown as mean ± standard deviation.

by one-way or two-way analysis of variance. The Wilcoxon signed-rank test was used to analyze nonparametric data. Significance was established at $P < 0.05$.

Results

Quantitative tissue measurements are reported in nanomolar concentrations of TUDCA within a given tissue, normalized to tissue weight. Quality controls indicated reliable measurements when concentrations were ≥1 nM, and all measurements below 1 nM were reported as measured, yet inconclusive. Data were analyzed after normalization using tissue weight compared with total protein, cholesterol, and other MS-detected reference molecules. Quality controls suggested that the levels by tissue weight were most reliable. Data derived from each delivery method at varying time points are shown in Table 1 (right globe) and Table 2 (left globe). IV delivery results were reported at the following time points (T = 0, 5, 30, and 60 minutes; Table 3).

Delivery Method

Oral Delivery

Twelve hours after the final dose on day 6, serum TUDCA concentrations were 217 and 242 (mean, 230 ± 18 nM). Levels in the neurosensory macula and peripheral retina measured 2.3 ± 0.4 and 1.9 ± 0.6 nM, respectively ($n = 2$ pigs, 4 eyes). Macular choroid levels and peripheral choroid levels were 2.9 ± 0.4 and 5.7 ± 2.1 nM, respectively, while vitreous levels were 30.8 ± 6 nM.

Intravenous Delivery

The first animal (T = 0 after completion of the infusion) had very high serum levels (104,000 nM), with low levels in the neurosensory macula (9.1 nM) and peripheral neurosensory retina (8.7 nM). Macular and peripheral choroid levels were higher (14.4 and 12.6 nM, respectively), and the vitreous was high (141.0 nM).

IV delivery (T = 5, 30, and 60 minutes) had the highest associated tissue levels in this study. Results were variable, so mean values were calculated. While vitreous level peaked at 30 minutes ($n = 1$ pig, 2 eyes; 1140 nM) and declined at 60 minutes, the mean ($n =$ 3 pigs, 6 eyes, and 3 time points) was 678 ± 413 nM. Similarly, the mean neurosensory macula level (252 ± 238 nM) and peripheral retina level (196 ± 171 nM) were high. The macular choroid and peripheral choroid levels were extremely high (1032 ± 1269 and 1219 ± 1486 nM, respectively). Levels after IV delivery are shown in Table 3.

IVitI Delivery

IVitIs are considered local delivery. Right (treated) and left globes were analyzed separately. Two animals (four globes) in each IVitI group were humanely killed

6 days after IVitI: 2 animals at 1 week; two animals at 2 weeks; and 2 animals at 4 weeks.

On day 6 ($n = 8$ globes), TUDCA levels were highest in the vitreous of the injected right eye, significantly higher than in the fellow left eye: 16.2 ± 6.1 vs. 0.5 ± 0.2 nM, respectively ($P = 0.01$). Vitreous levels on day 6 were much higher than in neurosensory macula (0.5 ± 0.5 nM; $P = 0.007$), macular choroid (1.3 ± 1.9 nM; $P = 0.01$), and peripheral neurosensory retina (3.3 ± 5.2 nM; $P = 0.04$).

Comparative data showed that TUDCA was present in the uninjected fellow left eye 4 weeks after injection of the right (Fig. 3). Peripheral choroid levels (15.3 ± 16.7 nM) exceeded those of macular choroid levels (1.3 ± 1.9 nM) ($P = 0.02$). Neurosensory macula (0.5 ± 0.5 nM) and peripheral neurosensory retina levels (3.3 ± 5.2 nM) were low. Thus, it appears that IvitIs diffuse to the vitreous, peripheral choroid, and peripheral neurosensory retina, with low and unreliable levels measured in the macular tissues.

In the right eye, at postinjection days 13 and 25, the only reliable (≥1 nM) tissue measurements were from the vitreous (1.3 and 2.0 nM, respectively) and peripheral choroid (2.9 ± 1.8 and 1.7 ± 0.5 nM, respectively). All other levels were undetectable or nearly undetectable. In the uninjected left eye, all measures were undetectable. Vitreous levels declined progressively with time while peripheral choroid levels peaked at 1 week.

Suprachoroidal Implant

Serum. The SCI group had higher systemic serum levels of TUDCA, both in the SCI-H (Fig. 4) and SCI-L (Fig. 5) groups, which peaked during the second week. Serum levels in the SCI-H group at 1, 2, and 4 weeks ($n = 5$, 4, and 5, respectively) after implantation were 8.9 ± 5.9, 45.4 ± 49.2, and 27.4 ± 35.3 nM. In the

Table 2. TUDCA Levels in Tissue Samples from the Left Eye

Delivery Method and Sample Time, Left Eye ($N = 43$)	Tissue Level, nM							
	Serum	Vitreous	Macula Retina	Macula Choroid	Peripheral Retina	Peripheral Choroid	Residual Retina	Residual Choroid
1 week								
IVitI ($n = 4$)	3.7 ± 2.5	0.5 ± 0.2	0.1 ± 0.2	0.3 ± 0.5	0.2 ± 0.2	0.1 ± 0.1	0.1 ± 0.2	0.5 ± 0.5
SCI-H ($n = 5$)	8.9 ± 5.9	1.9 ± 2.4	0.3 ± 0.5	0.1 ± 0.3	0.2 ± 0.3	0.7 ± 0.6	0.1 ± 0.3	0.3 ± 0.1
SCI-L ($n = 6$)	3.9 ± 5.7	0.8 ± 0.8	0.2 ± 0.3	0.6 ± 1.1	0.2 ± 0.2	0.0 ± 0.1	0.2 ± 0.2	0.2 ± 0.2
2 weeks								
IVitI ($n = 4$)	9.2 ± 4.8	0.6 ± 0.4	0.5 ± 0.3	0.2 ± 0.1	0.3 ± 0.3	1.1 ± 0.7	0.0 ± 0.0	0.5 ± 0.5
SCI-H ($n = 4$)	45.4 ± 49.2	0.2 ± 0.4	0.1 ± 0.1	0.9 ± 1.6	1.2 ± 1.9	0.8 ± 0.8	0.3 ± 0.3	1.0 ± 1.1
SCI-L ($n = 7$)	34.4 ± 45.6	0.4 ± 0.7	0.2 ± 0.2	0.4 ± 0.6	0.6 ± 1.1	0.3 ± 0.3	0.2 ± 0.2	0.5 ± 0.4
4 weeks								
IVitI ($n = 4$)	4.6 ± 4.6	3.9 ± 3.3	1.2 ± 2.4	0.6 ± 0.8	0.2 ± 0.4	2.0 ± 3.7	0.1 ± 0.1	0.4 ± 0.4
SCI-H ($n = 5$)	27.4 ± 35.3	1.4 ± 0.8	0.0 ± 0.1	0.1 ± 0.2	0.2 ± 0.2	0.0 ± 0.0	0.2 ± 0.3	0.4 ± 0.4
SCI-L ($n = 4$)	5.5 ± 3.8	0.1 ± 0.1	0.1 ± 0.1	0.2 ± 0.2	1.0 ± 1.8	0.2 ± 0.3	0.1 ± 0.1	0.1 ± 0.1

Data are shown as mean ± standard deviation.

Table 3. TUDCA Levels after Intravenous Delivery

Time from Injection	Tissue Level, nM							
	Serum	Vitreous	Macula Retina	Macula Choroid	Peripheral Retina	Peripheral Choroid	Residual Retina	Residual Choroid
T = 0	104,000	141.0	9.1	14.4	8.7	12.6	5.6	12.6
5 min	NA	550	132	426	98.2	485	117	528
30 min	NA	1,140	99.1	179	96.1	243	87.2	211
60 min	NA	344	526	2,490	393	2,930	841	6,760
Mean ± SD	NA	678 ± 413	252 ± 238	1032 ± 1269	196 ± 171	1219 ± 1486	348 ± 427	2500 ± 3693

NA, not applicable (specimens were either lost or not obtained);
T, time.

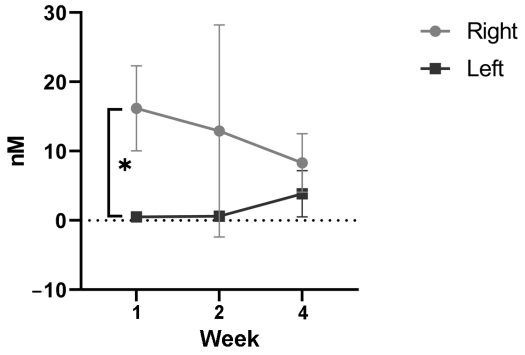

Figure 3. Intravitreal injection. The mean vitreous TUDCA levels in the right and left eyes after intravitreal delivery on day 6 ($n = 4$ pigs, 8 globes) were 16.2 ± 6.1 vs. 0.5 ± 0.2 nM, respectively (*$P = 0.01$). Although the drug levels in the right vitreous decreased slowly, by week 4, the mean TUDCA levels in the uninjected fellow left eyes increased to 3.9 ± 3.3 nM ($n = 4$ pigs, 8 eyes).

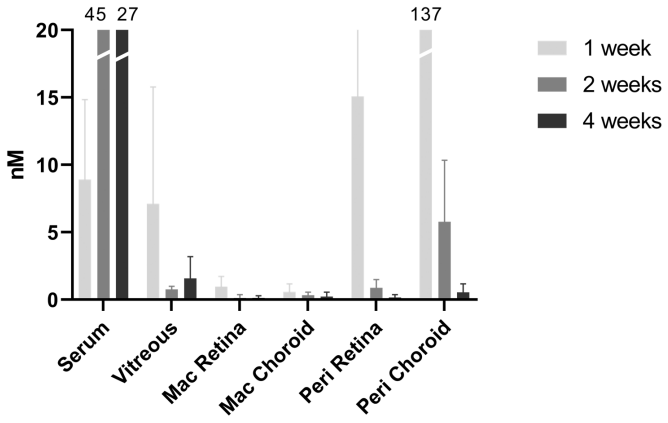

Figure 4. SCI-H. The mean TUDCA serum levels following SCI-H implantation peaked at 2 weeks (45.4 ± 49.2 nM; $n = 4$ pigs, 8 globes) and were significantly higher ($P < 0.007$) than in all other tissues (except the peripheral choroid). However, mean TUDCA levels in the macular neurosensory retina (1.0 ± 0.8 nM) and macular choroid (0.6 ± 0.6 nM) were significantly lower than serum, peripheral choroid, and peripheral neurosensory retinal levels ($P = 0.002$). Mac, macular; peri, peripheral.

SCI-L group ($n = 6$, 7, and 4 globes, respectively) at the same intervals, the serum levels were 3.9 ± 5.7, 34.4 ± 45.6, and 5.5 ± 3.8 nM. Thus, the 2-week interval was the peak serum level after SCI.

Neurosensory Macula

The only measurable TUDCA levels in the neurosensory macula occurred at 1 week after implantation in the SCI-H group ($n = 5$) and only in the right eye (1.0 ± 0.8 nM). All other measurements (SCI-H and SCI-L) were <1.0 nM (below the reliable quantitative limit of the mass spectroscopy). Macular choroid levels were also near zero. Thus, tissue measurements from fellow globes serve as a large control group for

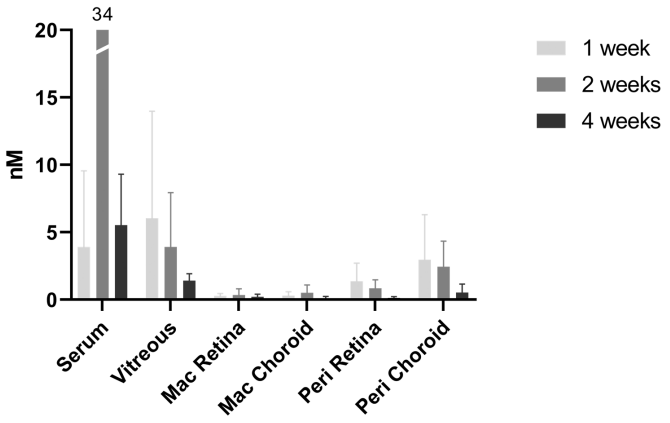

Figure 5. SCI-L. The mean TUDCA serum levels following SCI-L implantation peaked at 2 weeks (34.4 ± 45.6 nM; $n = 7$ pigs, 14 globes) and were significantly higher ($P < 0.001$) than in all other tissues, including the peripheral choroid. The 2-week mean TUDCA levels were as follows: vitreous (3.9 ± 4.0 nM), neurosensory macula (0.3 ± 0.5 nM), macular choroid (0.5 ± 0.6 nM), peripheral neurosensory retina (0.8 ± 0.6 nM), and peripheral choroid (2.4 ± 1.9 nM). Mac, macular; peri, peripheral.

this study, with reliable tissue levels measured at or near zero ($n = 116$ tissue specimens ≤1.0 nM).

Peripheral Overlying Neurosensory Retina and Choroid

Levels in the neurosensory retina directly over the SCI-H versus SCI-L implant 1 week after implantation ($n = 5$ and $n = 6$, respectively) were 15.1 ± 15.3 and 1.4 ± 1.4 nM, with the corresponding overlying choroid levels at 137 ± 207 and 3.0 ± 3.4 nM, respectively. For the SCI-H implant, this peripheral choroid TUDCA tissue level (137 ± 207 nM) was significantly higher than that of serum (8.9 ± 5.9 nM; $P = 0.004$), vitreous (7.1 ± 8.7 nM; $P = 0.003$), neurosensory macula (1.0 ± 0.8 nM; $P = 0.002$), macular choroid (0.6 ± 0.6 nM, $P = 0.002$), and peripheral neurosensory retina (15.1 ± 15.3 nM; $P = 0.007$).

At week 2, the SCI-H ($n = 5$) and SCI-L ($n = 7$) groups still had measurable peripheral overlying choroidal tissue levels (5.8 ± 4.6 and 2.4 ± 1.9 nM, respectively), even though the overlying retina levels had decreased to <1.0 nM. The levels in postimplant weeks 2 and 4 for the SCI groups were unmeasurable or <1.0 nM.

Vitreous

The SCI-H ($n = 5$) and SCI-L ($n = 6$) groups at 1 week were 7.1 ± 8.7 and 6.0 ± 7.9 nM, respectively. There was a progressive decrease in vitreous levels in the SCI-H and SCI-L implants. By week 2, there were minimal levels in both groups ($n = 11$; 2.8 ± 3.5 nM). By week 4, vitreous levels in the right eye ($n = 9$) were

Table 4. Serum Bile Acid Levels by Drug Delivery System

Delivery Method and Sample Time	Bile Acid, nM					
	TUDCA	CA	CDCA	DCA	LCA	UDCA
1 week						
Oral ($n = 2$)	230 ± 18	0 ± 0	9900 ± 283	41 ± 2.1	3115 ± 276	30,900 ± 5940
IVitI ($n = 4$)	3.7 ± 2.5	2.3 ± 4.5	22,699 ± 19,667	0 ± 0	1682 ± 1071	2176 ± 2678
SCI ($n = 10$)	6.0 ± 6.2	5.5 ± 17	3504 ± 2198	33.7 ± 52	874 ± 556	47.2 ± 126
2 weeks						
IVitI ($n = 4$)	9.1 ± 4.8	32 ± 19	47,425 ± 32,862	0 ± 0	1727 ± 1170	1817 ± 1364
SCI ($n = 12$)	35 ± 44	518 ± 608	51,203 ± 21,910	17,471 ± 26,751	4348 ± 3775	9256 ± 6971
4 weeks						
IVitI ($n = 4$)	4.6 ± 4.6	238 ± 179	46,675 ± 15,901	0 ± 0	1825 ± 1974	2134 ± 1907
SCI ($n = 11$)	23 ± 28	224 ± 251	40,436 ± 21,868	7965 ± 16,993	4272 ± 7010	6395 ± 9080

Data are shown as mean ± standard deviation. CA, cholic acid; CDCA, chenodeoxycholic acid; DCA, deoxycholic acid; LCA, lithocholic acid; UDCA, ursodeoxycholic acid.

1.6 ± 1.6 nM in the SCI-H group and 1.4 ± 0.5 nM in the SCI-L group. At week 4, vitreous levels were measurable at 1.4 ± 0.8 nM in the untreated fellow left eye in the SCI-H group ($n = 5$).

Serum Bile Acid Conjugates

The oral, IV, and SCI implants delivered TUDCA, yet substantial amounts of bile acid conjugates were detected in the serum and upregulated in response to TUDCA administration (Table 4). For example, cheno-, urso-, deoxy-, and lithocholic acid conjugates were found in high concentrations. Deoxycholic acid was not detected after intravitreal injections, although it was detected after other delivery methods.

Discussion

This pharmacokinetic study provides an important comparison of ocular drug tissue levels in a large animal model using both systemic and local delivery methods (oral, IV, IVitI, or SCI). We selected TUDCA because of its molecular similarities to triamcinolone, which has shown favorable pharmacokinetics in large animal models.[12] Also, TUDCA has been reported to have beneficial effects in numerous animal models of retinal degeneration.[26–28,30–36,38] The results for tissue levels of TUDCA after various delivery methods in a large animal model are important to determine the best approach for human clinical studies. Although bile acids are associated with some systemic adverse effects, most are related to gastrointestinal bile acid malabsorption, which occurs primarily in persons with irritable bowel syndrome.[37] The current study was neither large enough nor designed to detect specific adverse effects of TUDCA, yet it was well tolerated both systemically and locally within the eye for all different types of delivery. All animals had minimal postimplant ocular inflammation with no surgical complications, and all gained weight without the occurrence of clinically relevant diarrhea.

In prior animal studies, oral delivery doses reported by other authors are 500 mg/kg and given either intraperitoneally or subcutaneously.[26,28,34] In our study, oral dosing (70 mg/kg) was only slightly higher than the oral delivery (10 mg/kg) in human studies of retinal detachment.[39] The results from the human studies[39] suggest that there are measurable concentrations of bile acid from the subretinal and vitreous fluids. The highest tissue levels in our study were achieved with direct IV delivery. Compared to local delivery, IV administration led to a nearly 100 times higher neurosensory macular tissue level than local administration and 1000 times higher local tissue level in the macular and peripheral choroid. The choroid had 100 times higher concentrations than local delivery. Further studies would be required to demonstrate the safety of IV therapy for human studies. Although it is difficult to compare a 1-g immediate intravascular dose with any form of local delivery analyzed days or weeks later, immediate tissue analysis is only used to establish approximate tissue levels.

IVitIs were associated with very low levels of TUDCA in neurosensory macula (<0.5 nM). Macular choroid levels were near the lower detection limit (1.3 nM). On day 6 after IVitIs, peripheral choroid levels

were higher (15.3 nM) and peripheral retina levels were modest (3.3 nM), suggesting that TUDCA from the vitreous was diffusing from the eye via the peripheral choroidal blood flow. By 4 weeks after IVitIs, only low levels remained in the vitreous (1.6 nM) and peripheral choroid (2.6 nM), further supporting this theory. Serum levels peaked at week 2 after IVitI, then declined.

Overall local ocular tissue levels were low for the sustained-release, suprachoroidal implant, and this offers new insights into the tissue distribution of suprachoroidal drug delivery. Most important, delivery into the peripheral suprachoroidal space did not produce meaningful macular drug tissue levels, even with higher-dose delivery. At week 1, using the high-dose implant, only 1-nM concentrations in the neurosensory macula were detected, and no meaningful levels were detected in any other tissue. To expect delivery to the macular tissues from a peripherally placed suprachoroidal delivery system, the drug would, therefore, need to be very potent. However, peripheral choroidal levels were high (137 nM) in the high-dose group at 1 week, dropping to 5.8 nM concentrations at week 2 and minimal local choroidal tissue levels at week 4. The corresponding neurosensory retinal tissue levels were only meaningful in the high-dose group at 1 week (15.1 nM). Furthermore, the contralateral neurosensory retina, 180° away from the SCI, had approximately half the tissue concentration at week 1 (7.3 nM), thereafter decreasing to below our detection limit.

SCI-H delivered high local tissue levels at 1 week that decreased dramatically thereafter. Also, the extremely low macular TUDCA levels suggested that suprachoroidal drug delivery from the peripheral equatorial region of the globe most likely diffuses rapidly through the choroidal venous drainage system, summarized in Figure 6. Because the short posterior ciliary arteries enter near the macula, this pattern of blood flow from the macula (arterial) out through the vortex (venous) likely explains the diffusional kinetics for suprachoroidal drug delivery. Thus, drugs in the suprachoroidal space diffuse in parallel with the choroidal blood flow. This phenomenon supports earlier data reported in the pig model.[13] Microneedles that deliver drug to this same region are also likely to have similar pharmacokinetics.[14] To our knowledge, this study is the first to report tissue drug distribution for a sustained-release suprachoroidal implant. Therefore, direct macular drug delivery using this method is limited and the pharmacokinetics of a suprachoroidal implant are more optimal for treating peripheral disorders.

Our tissue analyses have identified numerous isoforms of bile acids that likely resulted from modifications of the acids during enterohepatic circulation.[40] We found higher serum levels of cheno-, urso-, deoxy-, and lithocholic acid conjugates during our analyses of TUDCA, so our local tissue measurements of TUDCA only may underestimate the sum effects of the bile acid environment. Furthermore, we cannot speculate on the basis of the data presented herein that such conjugates may or may not have a role in neuroprotection of retinal tissues. Our study was designed primarily as a drug tissue distribution analysis of TUDCA in a disease-free, large animal model. The pig model closely replicates the blood flow patterns of the human eye.

In summary, we were able to show high local tissue drug levels using systemic TUDCA delivery without detectable adverse effects. Furthermore, a single IV delivery achieved very high local tissue levels of TUDCA, whereas oral delivery had modest relative tissue levels. Using local delivery, we were able to determine that diffusion of TUDCA follows the choroidal blood flow with the highest levels found in the peripheral tissues and the lowest levels in the macula. This work has implications for optimizing local ocular drug delivery.

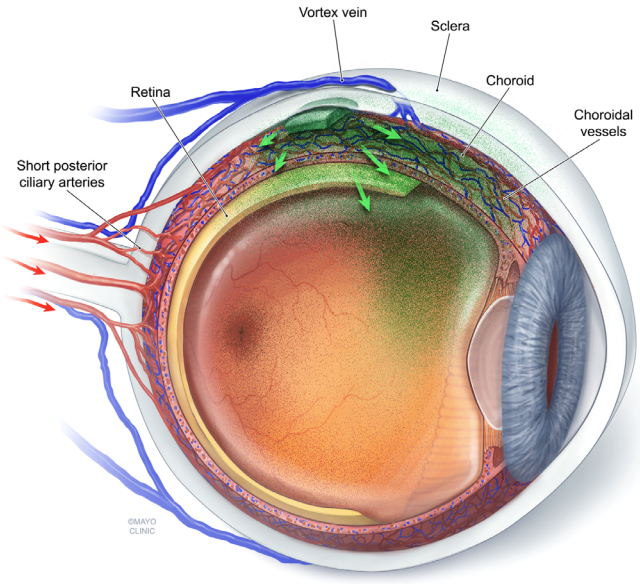

Figure 6. Globe schematic of a representative suprachoroidal, slow-release drug depot device (*green pellet*) eluting diffusible drug (*green*). Much of the drug diffuses into tissues surrounding the device, yet the choroidal blood flow pattern, from the short-posterior ciliary arteries through the macula and choroidal vasculature and out the vortex veins, leads to a diffusional flow that moves drug away from the macula and into the more peripheral and equatorial regions. (Used with permission by Mayo Foundation for Medical Education and Research.)

Acknowledgments

Supported by the Emory University School of Medicine; Abraham J. & Phyllis Katz Foundation, Shenandoah, Georgia; unrestricted grant from Research to Prevent Blindness, New York; Chungbuk National University; and the National Institutes of Health/National Eye Institute Core Grant P30 EY006360. The sponsor or funding organization had no role in the design or conduct of this research.

Portions of this study were presented at the annual meeting of the Association for Research in Vision in Ophthalmology, Vancouver, British Columbia, April 30, 2019 (Paper #3276).

Disclosure: **T.W. Olsen**, Emory University (P), iMacular Regeneration, LLC (I); **R.B. Dyer**, None; **F. Mano**, None; **J.H. Boatright**, Emory University (P); **M.A. Chrenek**, None; **D. Paley**, None; **K. Wabner**, None; **J. Schmit**, None; **J.B. Chae**, None; **J.T. Sellers**, None; **R.J. Singh**, None; **T.S. Wiedmann**, None

References

1. Nash BM, Wright DC, Grigg JR, Bennetts B, Jamieson RV. Retinal dystrophies, genomic applications in diagnosis and prospects for therapy. *Transl Pediatr*. 2015;4:139–163.
2. Russell S, Bennett J, Wellman JA, et al. Efficacy and safety of voretigene neparvovec (AAV2-hRPE65v2) in patients with RPE65-mediated inherited retinal dystrophy: a randomised, controlled, open-label, phase 3 trial. *Lancet*. 2017;390:849–860.
3. Ferris FL, III, Davis MD, Aiello LM. Treatment of diabetic retinopathy. *N Engl J Med*. 1999;341:667–678.
4. Brown DM, Kaiser PK, Michels M, et al. Ranibizumab versus verteporfin for neovascular age-related macular degeneration. *N Engl J Med*. 2006;355:1432–1444.
5. Rosenfeld PJ, Brown DM, Heier JS, et al. Ranibizumab for neovascular age-related macular degeneration. *N Engl J Med*. 2006;355:1419–1431.
6. Catt Research Group,Martin DF, Maguire MG, et al. Ranibizumab and bevacizumab for neovascular age-related macular degeneration. *N Engl J Med*. 2011;364:1897–1908.
7. Heier JS, Brown DM, Chong V, et al. Intravitreal aflibercept (VEGF trap-eye) in wet age-related macular degeneration. *Ophthalmology*. 2012;119:2537–2548.
8. Callanan DG, Gupta S, Boyer DS, et al. Dexamethasone intravitreal implant in combination with laser photocoagulation for the treatment of diffuse diabetic macular edema. *Ophthalmology*. 2013;120:1843–1851.
9. Tomkins-Netzer O, Lightman S, Drye L, et al. Outcome of treatment of uveitic macular edema: the multicenter uveitis steroid treatment trial 2-year results. *Ophthalmology*. 2015;122:2351–2359.
10. da Cruz L, Dorn JD, Humayun MS, et al. Five-year safety and performance results from the Argus II Retinal Prosthesis System Clinical Trial. *Ophthalmology*. 2016;123:2248–2254.
11. Einmahl S, Savoldelli M, D'Hermies F, Tabatabay C, Gurny R, Behar-Cohen F. Evaluation of a novel biomaterial in the suprachoroidal space of the rabbit eye. *Invest Ophthalmol Vis Sci*. 2002;43:1533–1539.
12. Olsen TW, Feng X, Wabner K, et al. Cannulation of the suprachoroidal space: a novel drug delivery methodology to the posterior segment. *Am J Ophthalmol*. 2006;142:777–787.
13. Olsen TW, Feng X, Wabner K, Csaky K, Pambuccian S, Cameron JD. Pharmacokinetics of pars plana intravitreal injections versus microcannula suprachoroidal injections of bevacizumab in a porcine model. *Invest Ophthalmol Vis Sci*. 2011;52:4749–4756.
14. Patel SR, Lin AS, Edelhauser HF, Prausnitz MR. Suprachoroidal drug delivery to the back of the eye using hollow microneedles. *Pharm Res*. 2011;28:166–176.
15. Tran J, Craven C, Wabner K, et al. A pharmacodynamic analysis of choroidal neovascularization in a porcine model using three targeted drugs. *Invest Ophthalmol Vis Sci*. 2017;58:3732–3740.
16. Olsen TW. The suprachoroidal delivery route and exploring the potential of cell-based therapies for age-related macular degeneration. *Invest Ophthalmol Vis Sci*. 2018;59:321.
17. Bakri SJ, Thorne JE, Ho AC, et al. Safety and efficacy of anti-vascular endothelial growth factor therapies for neovascular age-related macular degeneration: a report by the American Academy of Ophthalmology. *Ophthalmology*. 2019;126:55–63.
18. Yamada N, Olsen TW. Routes for drug delivery to the retina: topical, transscleral, suprachoroidal and intravitreal gas phase delivery. *Dev Ophthalmol*. 2016;55:71–83.
19. Olsen TW. Suprachoroidal drug delivery: unique new observations. *Invest Ophthalmol Vis Sci*. 2015;56:4976.

20. Gu B, Liu J, Li X, Ma Q, Shen M, Cheng L. Real-time monitoring of suprachoroidal space (SCS) following SCS injection using ultra-high resolution optical coherence tomography in guinea pig eyes. *Invest Ophthalmol Vis Sci*. 2015;56: 3623–3634.
21. Rai Udo J, Young SA, Thrimawithana TR, et al. The suprachoroidal pathway: a new drug delivery route to the back of the eye. *Drug Discov Today*. 2015;20:491–495.
22. Gilger BC, Abarca EM, Salmon JH, Patel S. Treatment of acute posterior uveitis in a porcine model by injection of triamcinolone acetonide into the suprachoroidal space using microneedles. *Invest Ophthalmol Vis Sci*. 2013;54:2483–2492.
23. Rodrigues CM, Spellman SR, Sola S, et al. Neuroprotection by a bile acid in an acute stroke model in the rat. *J Cereb Blood Flow Metab*. 2002;22:463–471.
24. Castro RE, Sola S, Ramalho RM, Steer CJ, Rodrigues CM. The bile acid tauroursodeoxycholic acid modulates phosphorylation and translocation of bad via phosphatidylinositol 3-kinase in glutamate-induced apoptosis of rat cortical neurons. *J Pharmacol Exp Ther*. 2004;311:845–852.
25. Xavier JM, Rodrigues CM, Sola S. Mitochondria: major regulators of neural development. *Neuroscientist*. 2016;22:346–358.
26. Boatright JH, Moring AG, McElroy C, et al. Tool from ancient pharmacopoeia prevents vision loss. *Mol Vis*. 2006;12:1706–1714.
27. Drack AV, Dumitrescu AV, Bhattarai S, et al. TUDCA slows retinal degeneration in two different mouse models of retinitis pigmentosa and prevents obesity in Bardet-Biedl syndrome type 1 mice. *Invest Ophthalmol Vis Sci*. 2012;53:100–106.
28. Fernandez-Sanchez L, Lax P, Pinilla I, Martin-Nieto J, Cuenca N. Tauroursodeoxycholic acid prevents retinal degeneration in transgenic P23H rats. *Invest Ophthalmol Vis Sci*. 2011;52:4998–5008.
29. Fu Y, Zhang T. Pathophysiological mechanism and treatment strategies for Leber congenital amaurosis. *Adv Exp Med Biol*. 2014;801:791–796.
30. Lawson EC, Bhatia SK, Han MK, et al. Tauroursodeoxycholic acid protects retinal function and structure in rd1 mice. *Adv Exp Med Biol*. 2016;854:431–436.
31. Mantopoulos D, Murakami Y, Comander J, et al. Tauroursodeoxycholic acid (TUDCA) protects photoreceptors from cell death after experimental retinal detachment. *PLoS One*. 2011;6:e24245.
32. Oshitari T, Bikbova G, Yamamoto S. Increased expression of phosphorylated c-Jun and phosphorylated c-Jun N-terminal kinase associated with neuronal cell death in diabetic and high glucose exposed rat retinas. *Brain Res Bull*. 2014;101:18–25.
33. Oveson BC, Iwase T, Hackett SF, et al. Constituents of bile, bilirubin and TUDCA, protect against oxidative stress-induced retinal degeneration. *J Neurochem*. 2011;116:144–153.
34. Phillips MJ, Walker TA, Choi HY, et al. Tauroursodeoxycholic acid preservation of photoreceptor structure and function in the rd10 mouse through postnatal day 30. *Invest Ophthalmol Vis Sci*. 2008;49:2148–2155.
35. Xia H, Nan Y, Huang X, Gao J, Pu M. Effects of Tauroursodeoxycholic acid and alpha-lipoic-acid on the visual response properties of cat retinal ganglion cells: an in vitro study. *Invest Ophthalmol Vis Sci*. 2015;56:6638–6645.
36. Zhang T, Baehr W, Fu Y. Chemical chaperone TUDCA preserves cone photoreceptors in a mouse model of Leber congenital amaurosis. *Invest Ophthalmol Vis Sci*. 2012;53:3349–3356.
37. Camilleri M, Nadeau A, Tremaine WJ, et al. Measurement of serum 7alpha-hydroxy-4-cholesten-3-one (or 7alphaC4), a surrogate test for bile acid malabsorption in health, ileal disease and irritable bowel syndrome using liquid chromatography-tandem mass spectrometry. *Neurogastroenterol Motil*. 2009;21:e734–e743.
38. Boatright JH, Nickerson JM, Moring AG, Pardue MT. Bile acids in treatment of ocular disease. *J Ocul Biol Dis Infor*. 2009;2:149–159.
39. Daruich A, Picard E, Zola M, Henry H, Boatright JH, Behar-Cohen FF. Adjuvant ursodeoxycholic acid for retinal detachment: a potential neuroprotective therapy. *Invest Ophthalmol Vis Sci*. 2019;60:2795.
40. Chiang JY. Bile acids: regulation of synthesis. *J Lipid Res*. 2009;50:1955–1966.